Supporting Information

Mitochondrial-Localized Versus Cytosolic Intracellular CO-Releasing Organic PhotoCORMs: Evaluation of CO Effects Using Bioenergetics

Tatiana Soboleva,[†] Hector J. Esquer,[‡] Stacey N. Anderson,[†] Lisa M. Berreau[†*] and Abby D. Benninghoff[‡*]

[†]Department of Chemistry and Biochemistry, Utah State University, Logan, Utah 84322-0300, United States.

[‡]Department of Animal, Dairy and Veterinary Sciences, Utah State University, Logan, Utah 84322-4815, United States.

Contact Information:
Lisa M. Berreau
Lisa.berreau@usu.edu

Abby D. Benninghoff
Abby.Benninghoff@usu.edu

Table of Contents

Synthesis of 3-hydroxy-2-(4-carboxy)phenyl-benzo[*g*]chromen-4-one (1a). Sodium hydroxide (2.74 mL, 5 M, 13.5 mmol) was added to a suspension of 1-(3-hydroxynaphthalen-2-yl)ethanone[1] (0.420 g, 2.26 mmol) in ethanol (4.67 mL) and the mixtures was allowed to stir for 30 minutes at room temperature. 4-formyl benzoic acid (0.339 g, 2.26 mmol) was then added to the reaction and the resulting mixture was stirred for 5 hours at room temperature. The reaction was then cooled to 0°C in an ice bath, and hydrogen peroxide (2.00 mL, 30%) was added dropwise. The resulting mixture was stirred overnight while warming to room temperature. Acidification of the solution to pH = 6.5 with 0.5 M HCl resulted in the formation of a bright yellow precipitate which was isolated by filtration and washed with cold ethanol (0.300 g, 40%). ^{1}H NMR (CD_3OD, 500 MHz) δ 8.82 (s, 1H), 8.43 (d, *J* = 8.5 Hz, 2H), 8.22 (s, 1H), 8.15 (d, *J* = 8.5 Hz, 2H), 8.12 (d, *J* = 8.5 Hz, 1H), 8.04 (d, *J* = 8.5 Hz, 1H), 7.65 (t, *J* = 8.5 Hz, *J* = 8.0 Hz, 1H), 7.55 (t, *J* = 8.5 Hz, *J* = 8.0 Hz, 1H). FTIR (KBr, cm^{-1}) 3380 (br, ν_{O-H}), 1632 ($\nu_{C=O}$), and 1584 (ν_{C-O}). UV-vis (CH_3CN:DMSO (10:1), nm) (ε, M^{-1} cm^{-1}) 414 (11.4 ± 0.1 x 10^3), 394 (11.4 ± 0.2 x 10^3), 347 (13.5 ± 0.2 x 10^3). ESI/APCI-MS calcd. for $C_{20}H_{12}O_5$ $[MH]^+$: 333.0700; found: 333.0765 (100%). Anal. Calc. for $C_{20}H_{12}O_5$: C, 64.71, H, 3.64. Found: C, 64.55, H, 3.74.

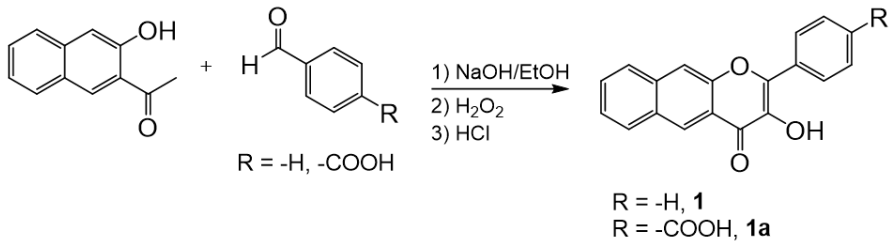

Scheme S1. The outline of synthesis for compounds **1**[2] and **1a**.

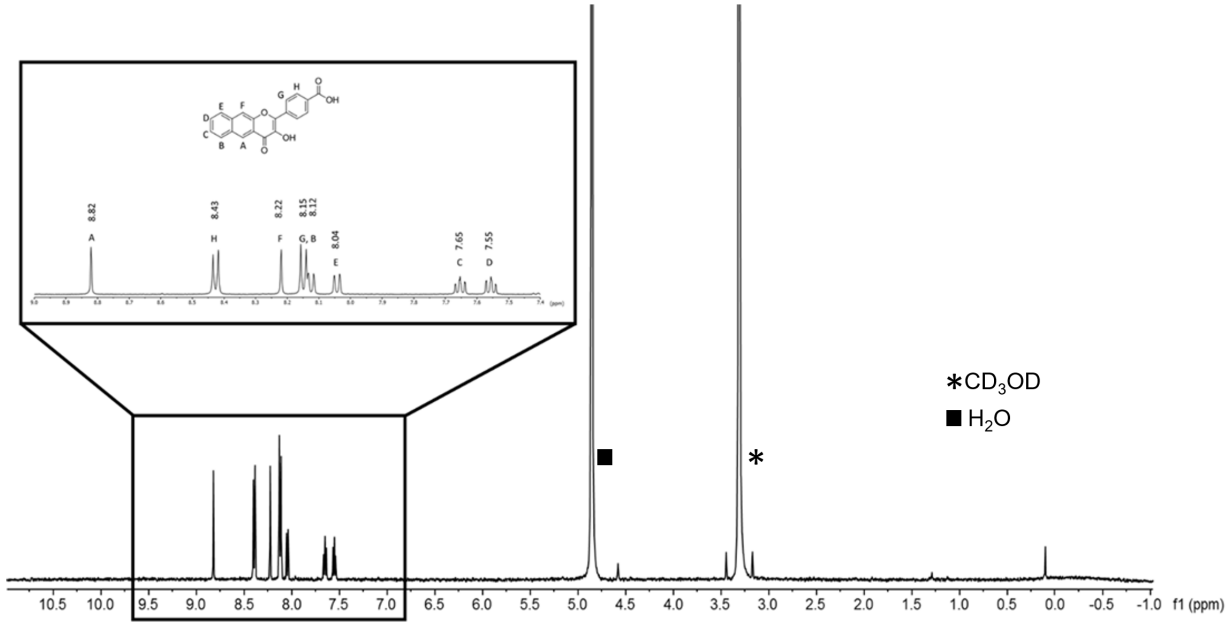

Figure S1. ^{1}H NMR of **1a** in CD_3OD. Assignment of resonances was based on comparison to **1**.

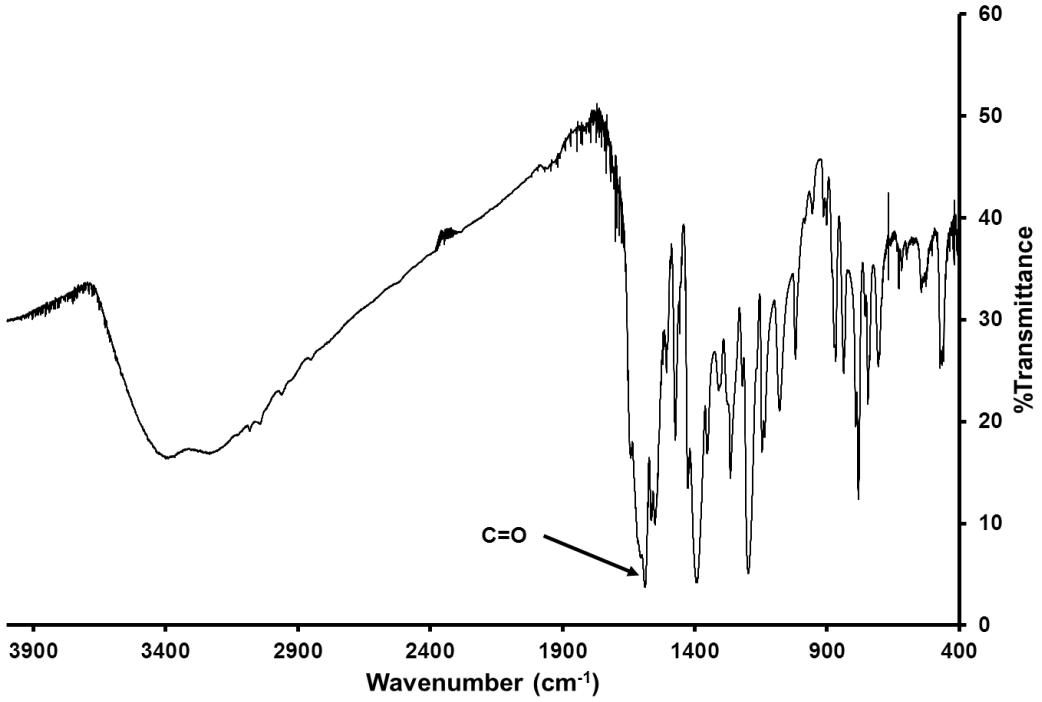

Figure S2. FT-IR spectrum of **1a** in KBr.

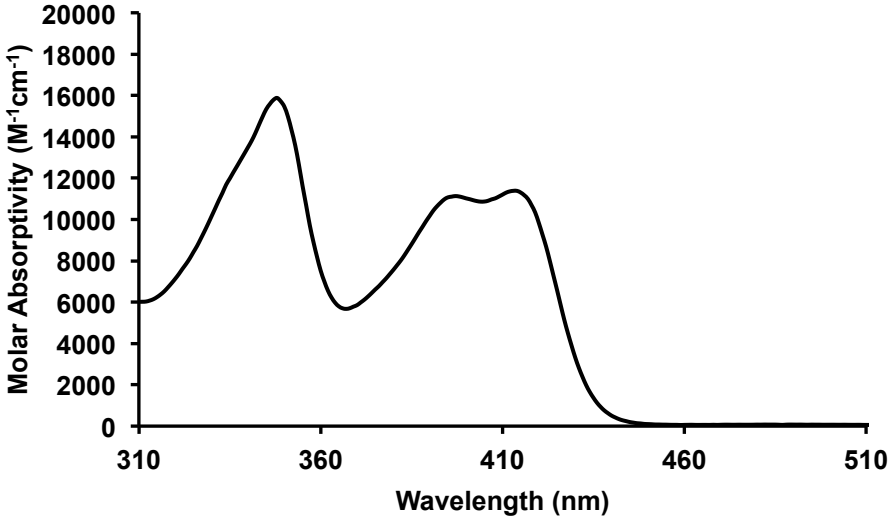

Figure S3. Absorption spectrum of **1a** in CH_3CN:DMSO (10:1).

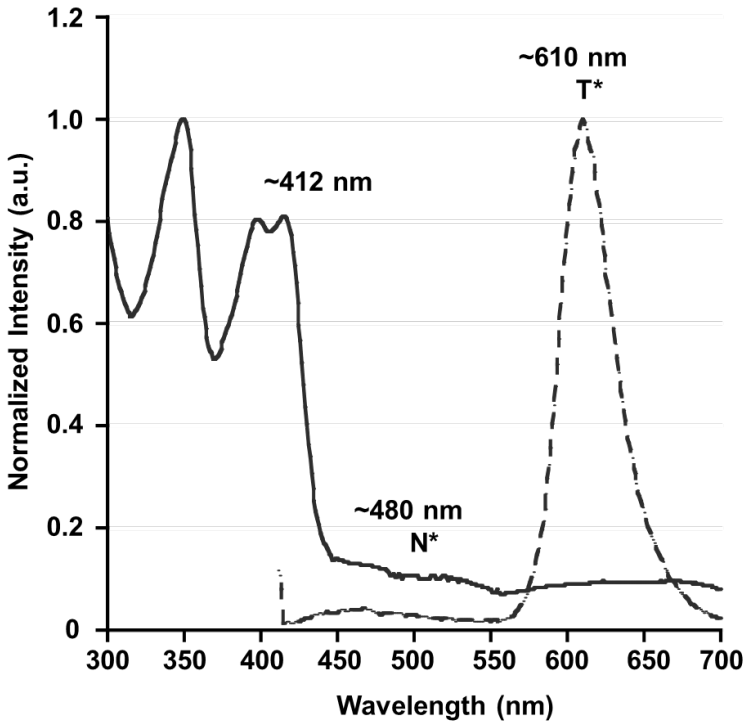

Figure S4. Overlay of normalized lowest energy absorption features of **1a** with its emission spectrum both of which were obtained in CH_3CN:DMSO (10:1). The emission features at ~480 nm and ~610 nm represent normal (N*) and tautomeric (T*) excited state forms of the flavonol, respectively.

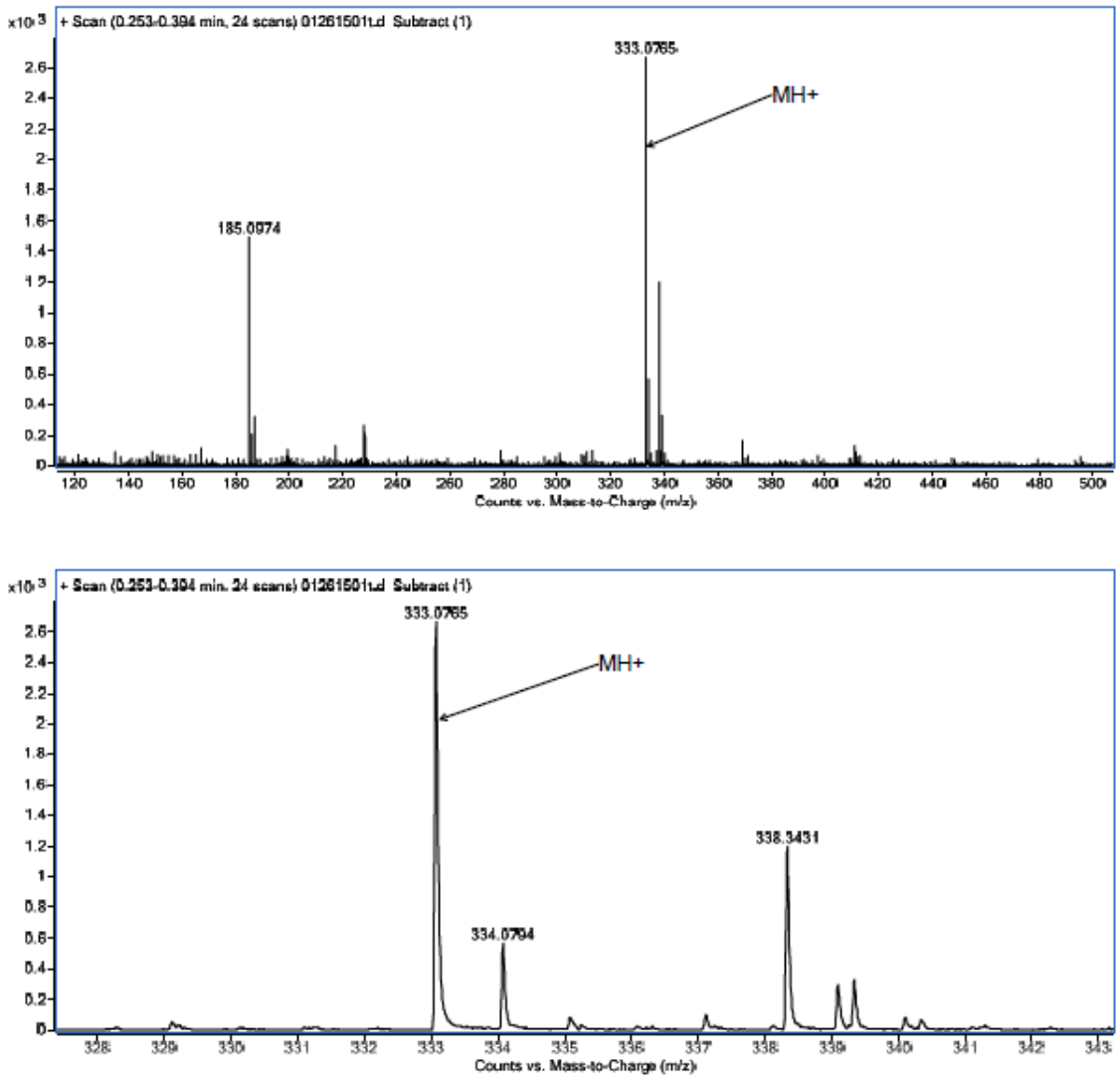

Measured Mass	333.0765	
Element	Low Limit	High Limit
C	15	25
H	5	25
O	3	7

Formula	Calculated Mass	mDaError	ppmError	RDB
C20 H13 O5	333.0758	0.7	2.3	14.5

Figure S5. ESI/APCI-MS of **1a**.

Characterization of 2 and 3

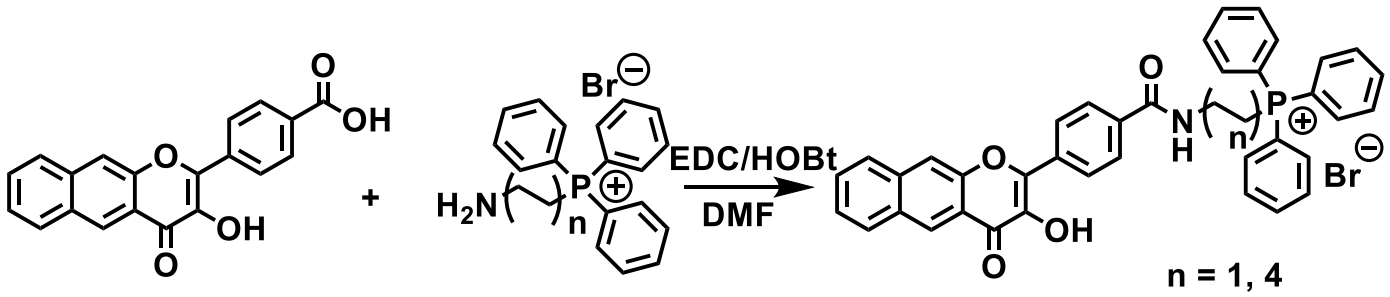

Scheme S2. General procedure of triphenylphosphonium tail coupling to the flavonol moiety.

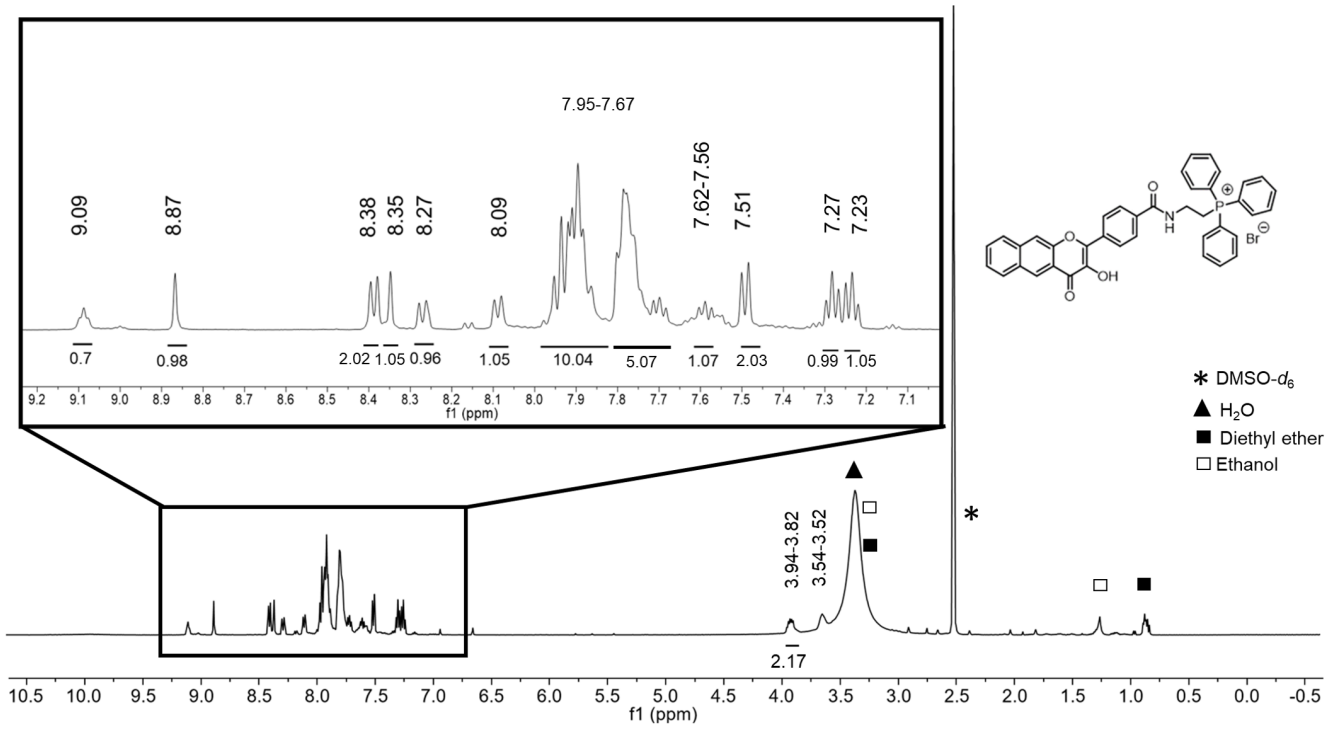

Figure S6. ^{1}H NMR of **2** in DMSO-d_6.

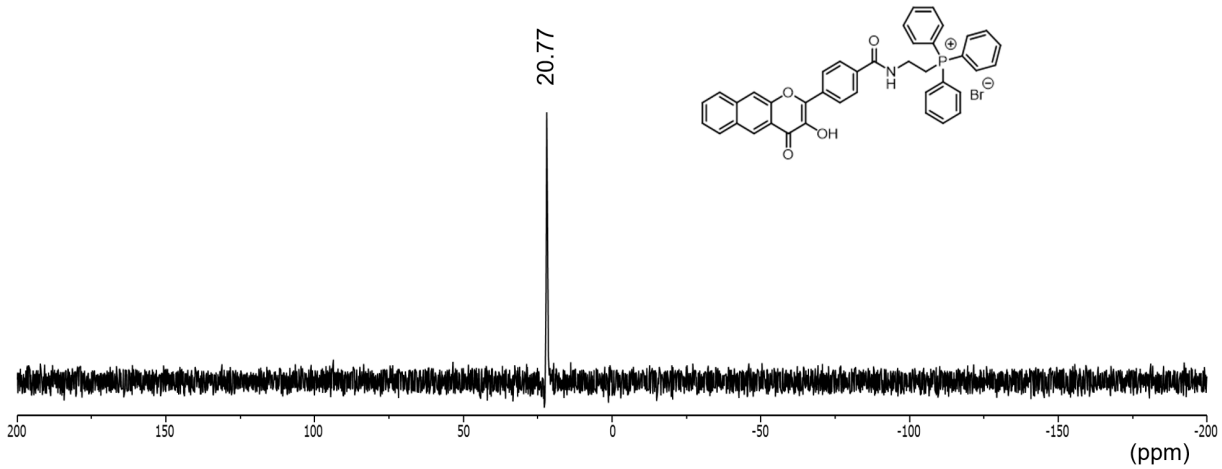

Figure S7. ^{31}P NMR of **2** in DMSO-d_6.

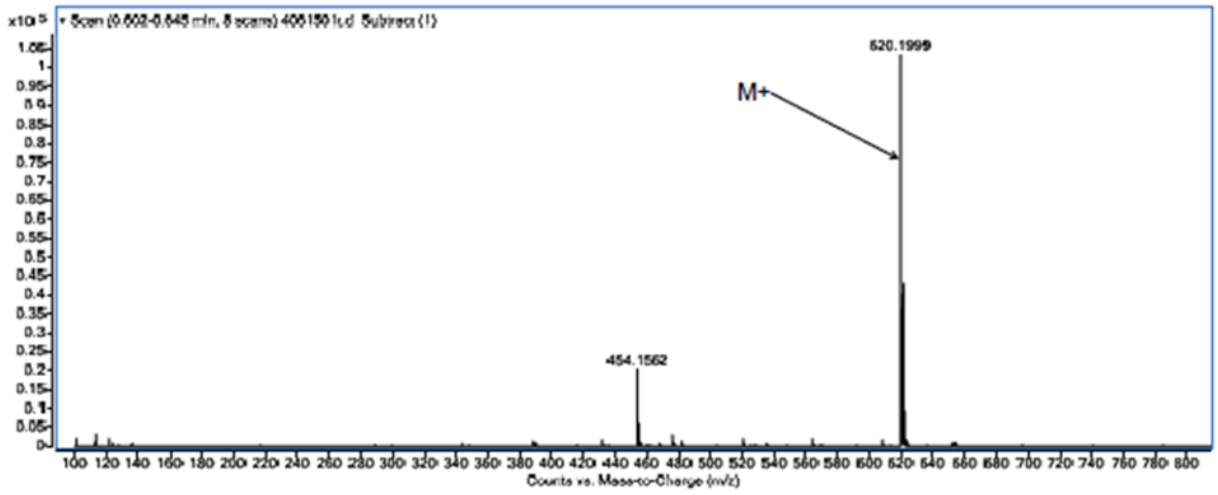

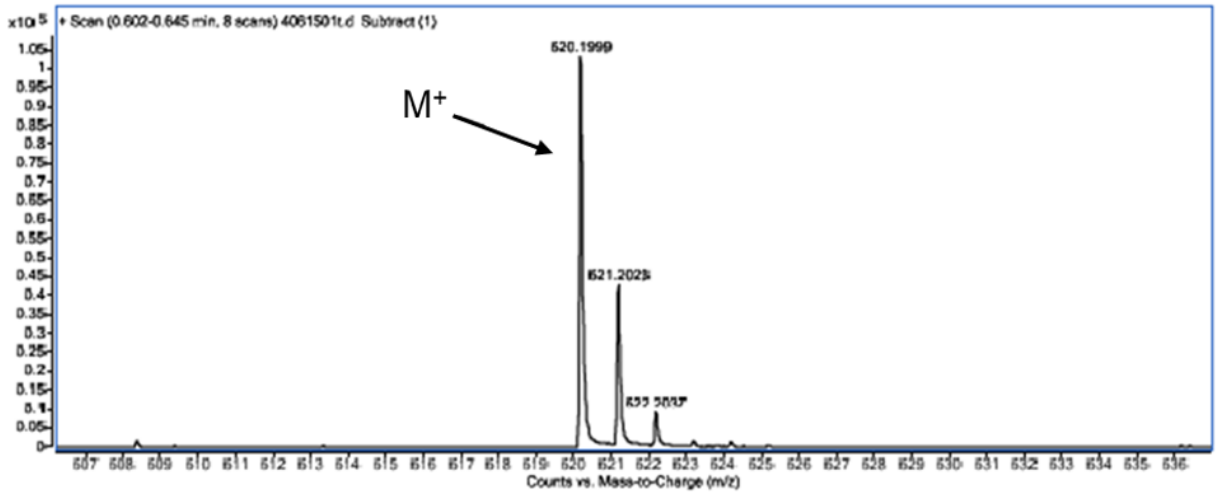

Measured Mass	620.1999	
Element	Low Limit	High Limit
C	35	45
H	20	40
N	0	2
O	2	6
P	0	1

Formula	Calculated Mass	mDaError	ppmError	RDB
C40 H31 N O4 P	620.1985	1.4	2.2	26.5
C44 H28 O4	620.1982	1.7	2.7	31

Figure S8. ESI/APCI-MS of **2**.

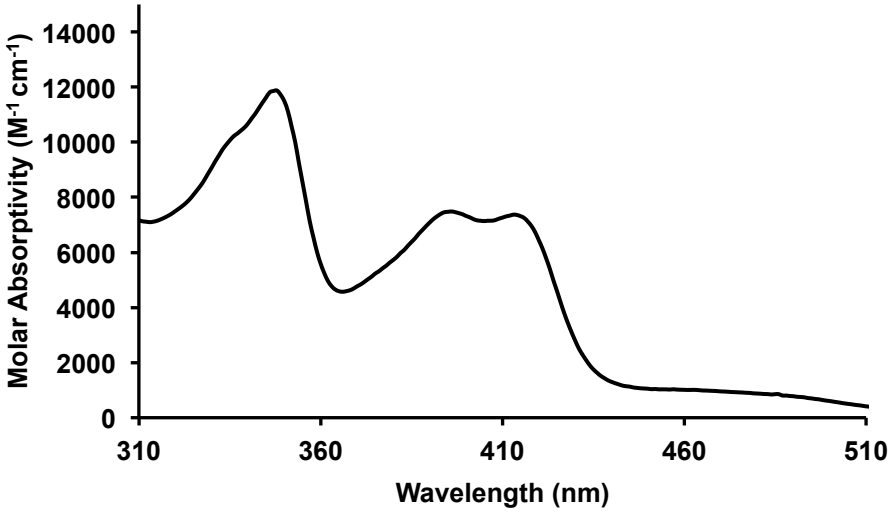

Figure S9. Absorption spectrum of **2** in CH_3CN:DMSO (10:1).

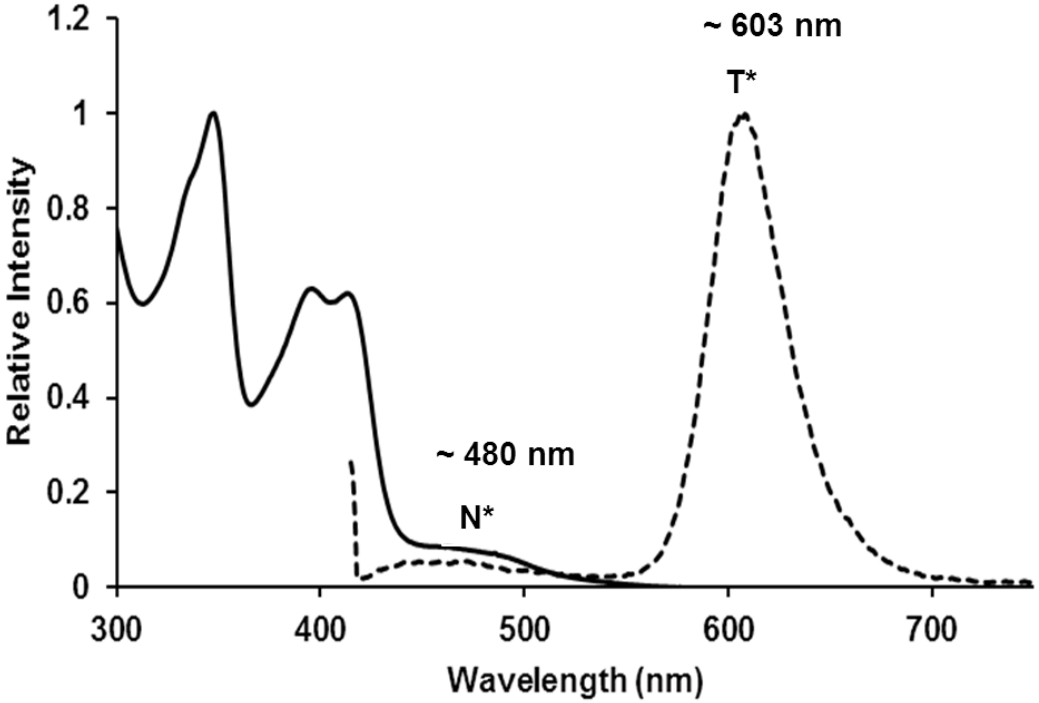

Figure S10. Overlay of normalized lowest energy absorption feature of **2** with the emission spectrum in CH_3CN:DMSO (10:1). Emission features at ~480 nm and ~603 nm represent normal (N*) and tautomeric (T*) excited forms.

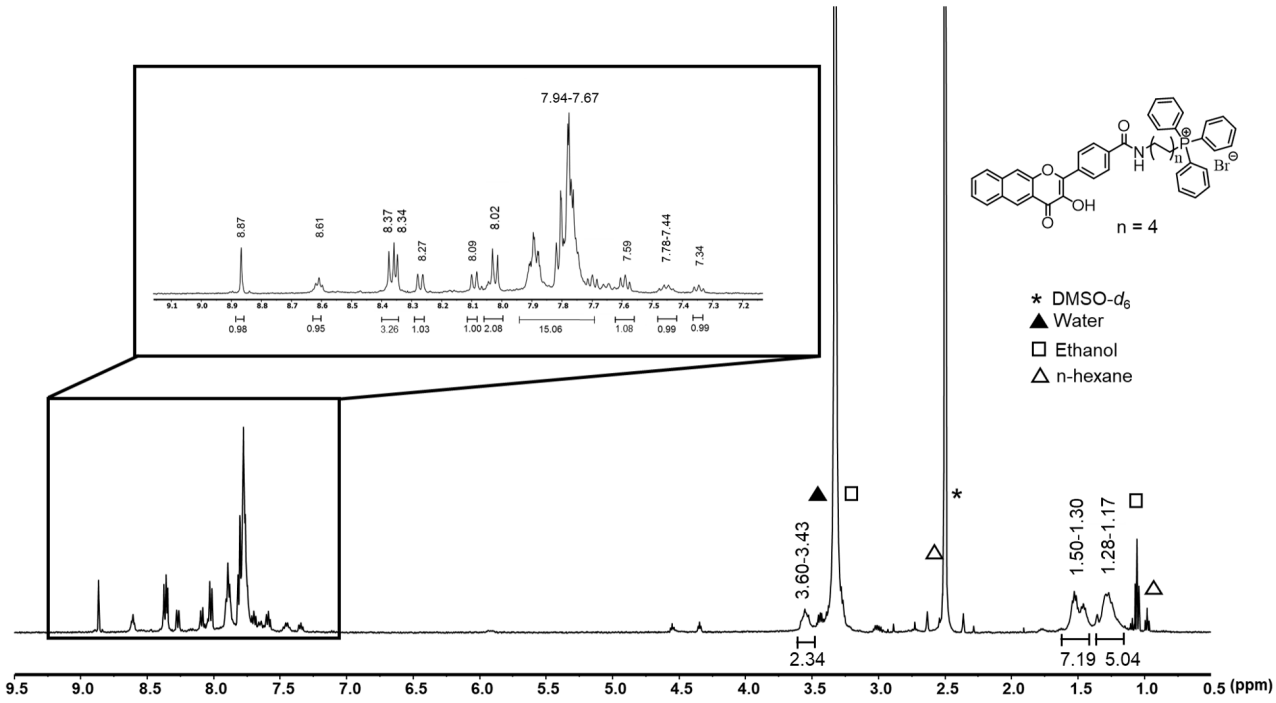

Figure S11. ^{1}H NMR of **3** in DMSO-d_6.

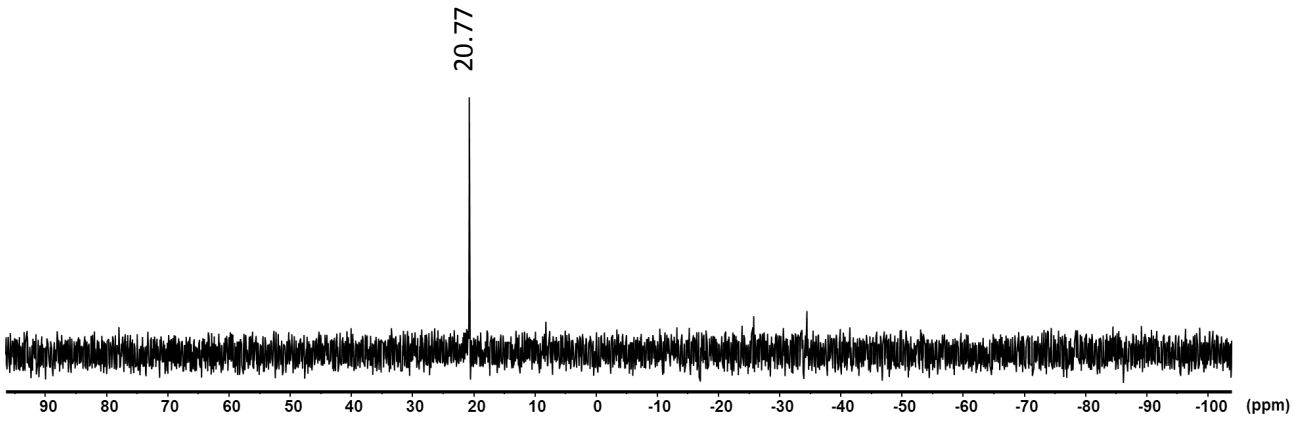

Figure S12. ^{31}P NMR of **3** in MeOH-d_4.

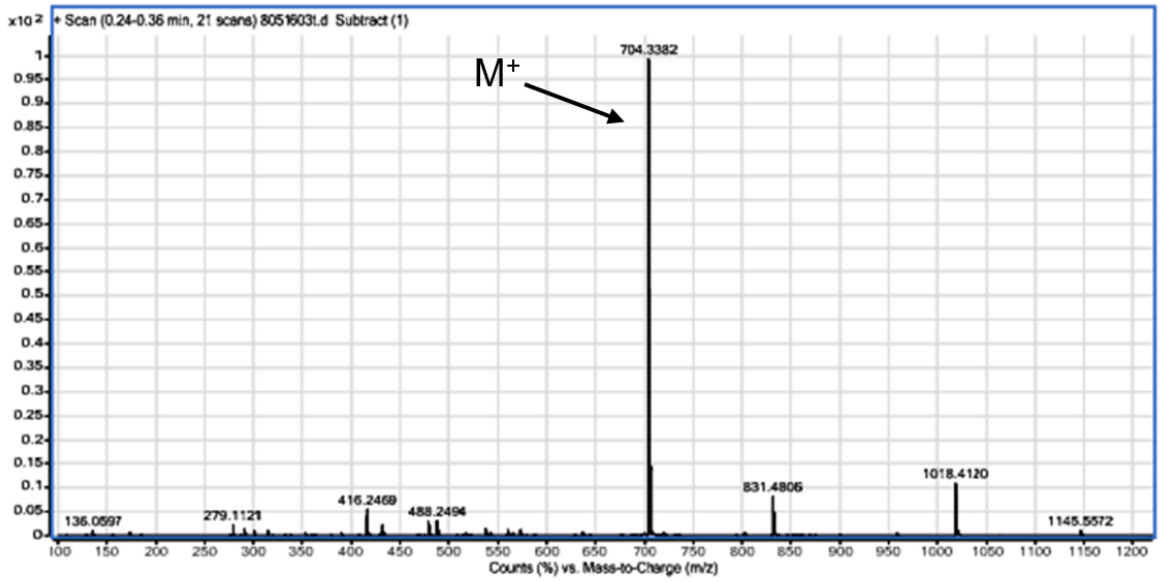

Figure S13. ESI/APCI-MS of **3**.

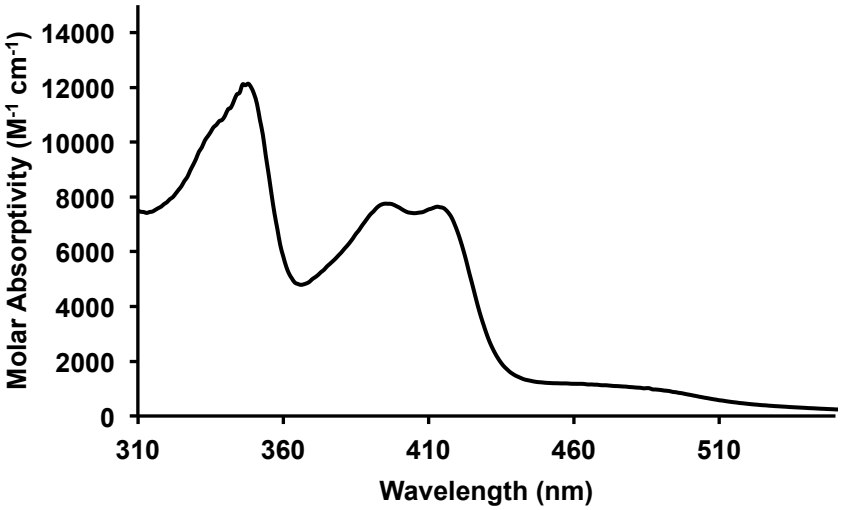

Figure S14. Absorption spectrum of **3** in CH_3CN:DMSO (10:1).

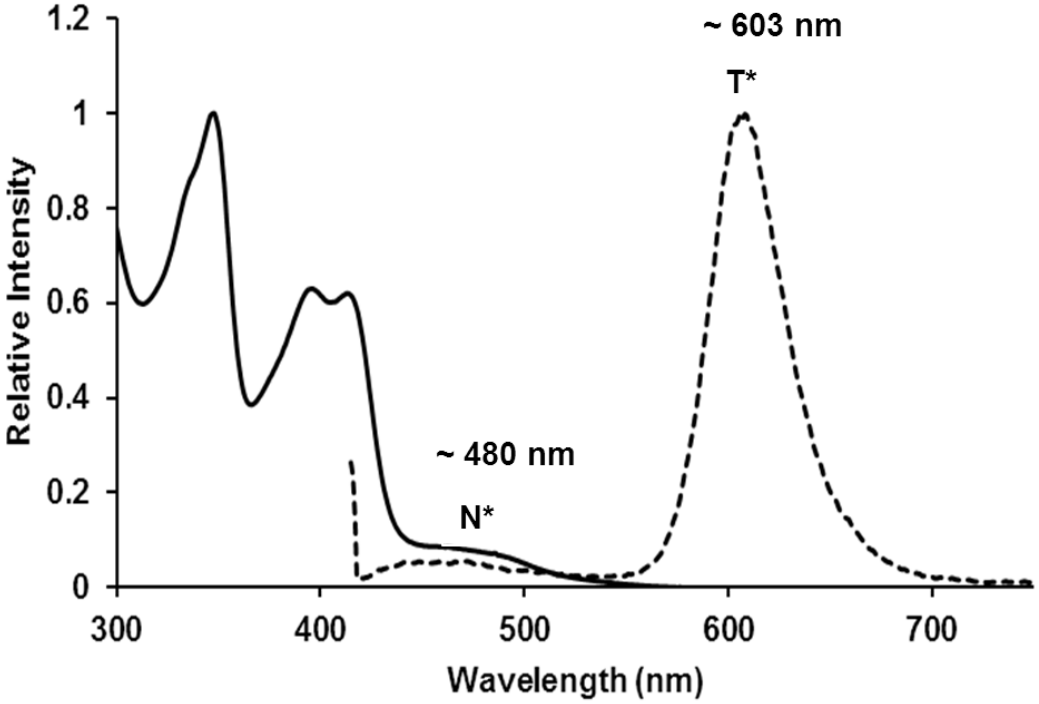

Figure S15. Overlay of normalized lowest energy absorption feature of **3** with the emission spectrum in CH_3CN:DMSO (10:1). Emission features at ~480 nm and ~603 nm represent normal (N*) and tautomeric (T*) excited forms.

Photoreactivity of 2 and 3 in the presence of oxygen; absorption and emission studies. A stock solution of **2** or **3** (3 mM) was prepared in DMSO for the subsequent UV-vis studies. Using the prepared stock solution, a UV-vis/fluorescence sample with a final flavonol concentration of 0.1 mM in a total of 3 mL of DMSO was prepared in a quartz cuvette with 1 cm path length. Initial absorption and emission spectra were taken for subsequent comparison. Then these samples were subjected to illumination at 419 nm for 24 hours. The reaction was determined complete as evidenced by the disappearance of the lowest energy absorption band of compound **2**.

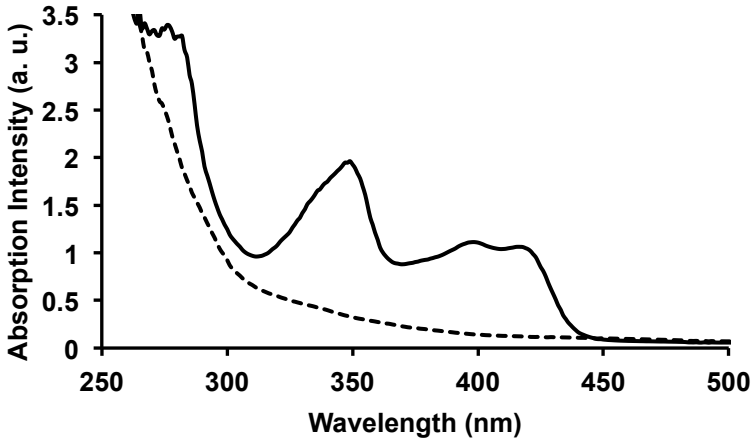

Figure S16. Absorption spectra of **2** prior (solid black line) and post (dotted black line) illumination in DMSO under air.

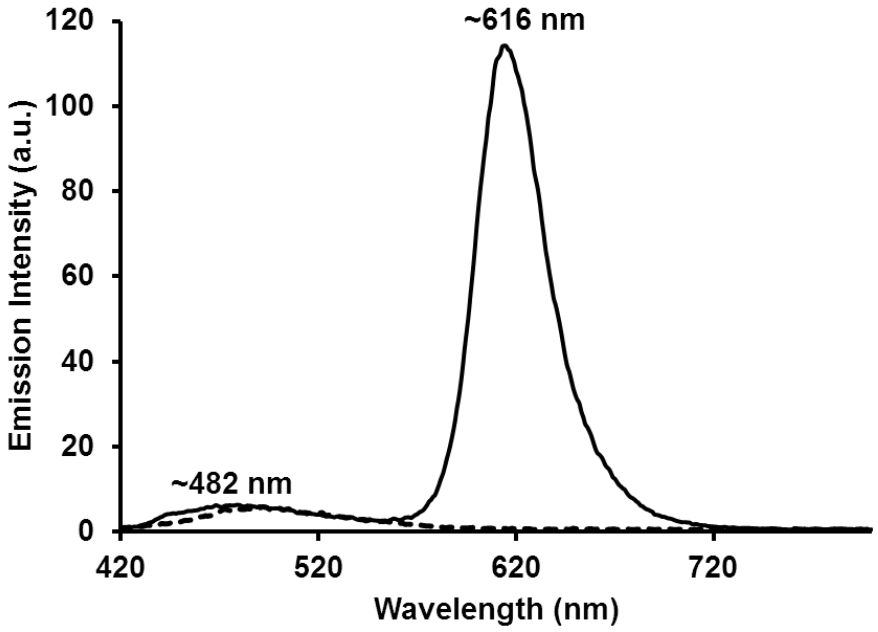

Figure S17. Emission of **2** prior (solid black line) and post (dotted black line) illumination in DMSO under air, generated upon excitation into the lowest energy absorption maximum.

Photoinduced CO release of 2 under air; NMR-tube experiment. A solution of **2** (~0.021 mmol) in ~1 mL DMSO-d_6 was placed in an NMR tube under air. An initial ^{1}H NMR spectrum was obtained. This NMR tube was then placed in a Rayonet photoreactor equipped with 419 nm lamps (8 lamps, light intensity 2450 lx) and was illuminated for 24 hours. The solvent was then removed via lyophilization conditions yielding a dark orange solid. ^{1}H NMR (DMSO-d_6, 500 Hz) δ 9.01 (s, 1H), 8.27 (s, 1H), 8.01 (d, J = 8.0 Hz, 1H), 7.95-7.68 (m, 15H), 7.63 (d, J = 8.2 Hz, 2H), 7.57 (d, J = 7.9 Hz, 1H), 7.46-7.42 (m, 2H), 7.37-7.34 (m, 3H), 6.93 (s, 1H), 3.94-3.82 (m, 2H), 3.54-3.52 (m, 2H), ppm. ESI/APCI-MS (relative intensity) calcd. for $C_{39}H_{31}BrNO_5P$ $[M]^+$: 620.1985; found $[M]^+$: 454.1504. The molecular ion for **4** was not identified. However, a fragment corresponding to the TPP tail with flavonol B-ring.

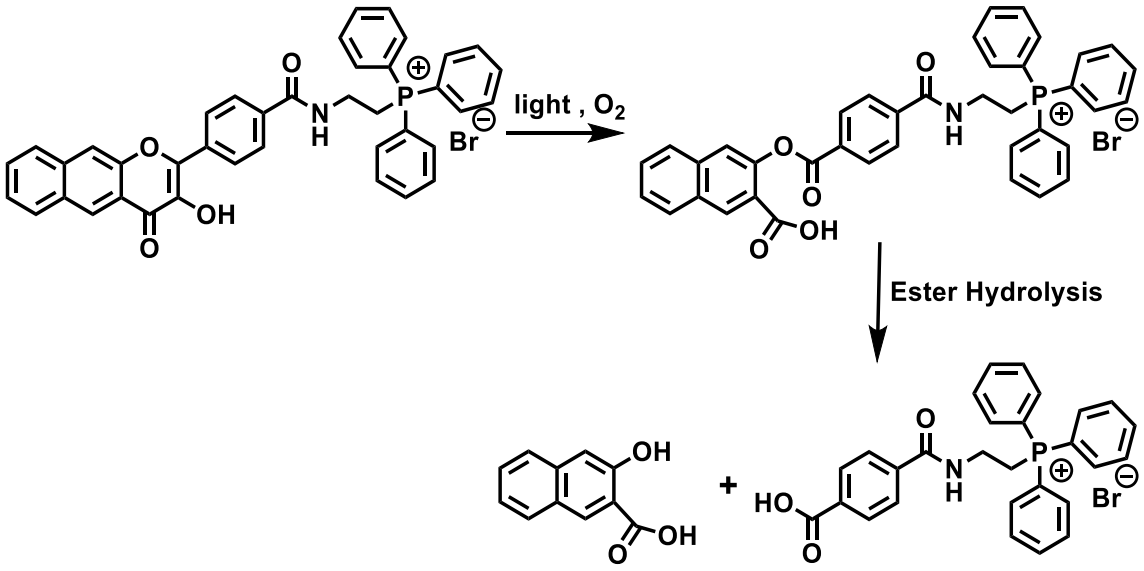

Scheme S3. Photoinduced CO release reaction of **2** to produce **4**.

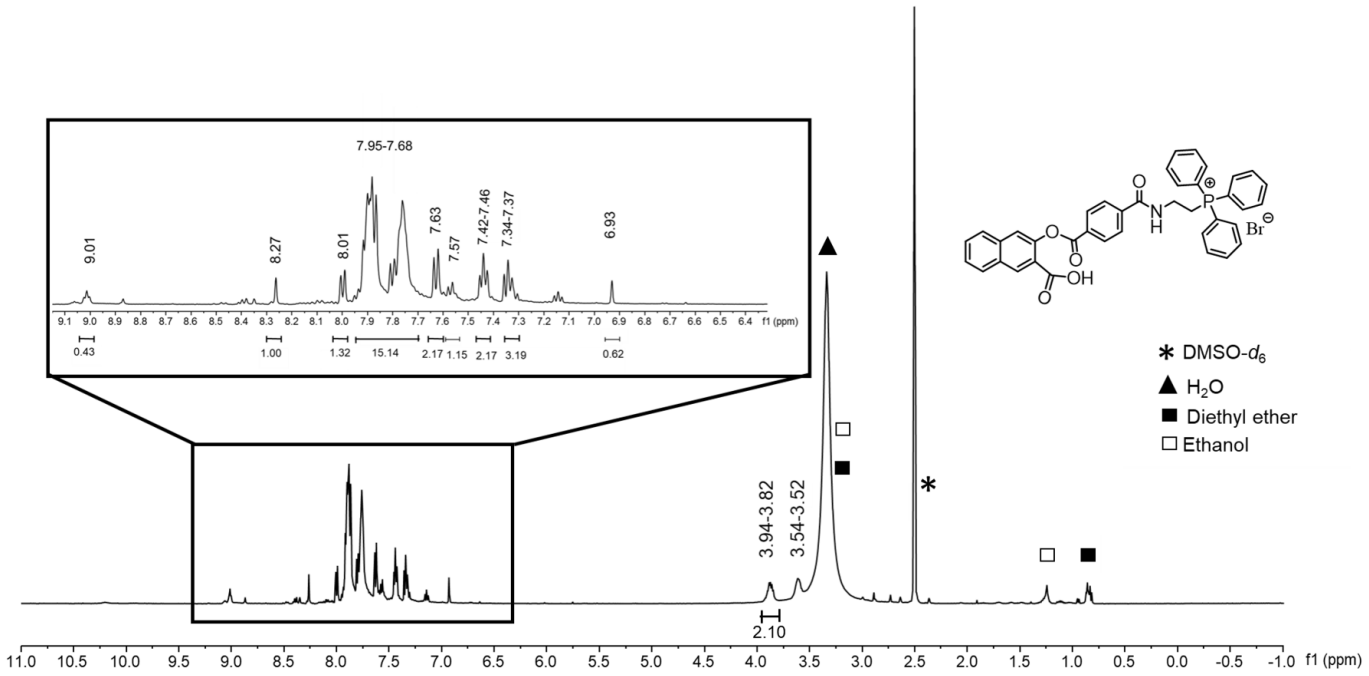

Figure S18. ^{1}H NMR of **2** in DMSO-d_6 illuminated at 419 nm for 24 hours to produce **4**.

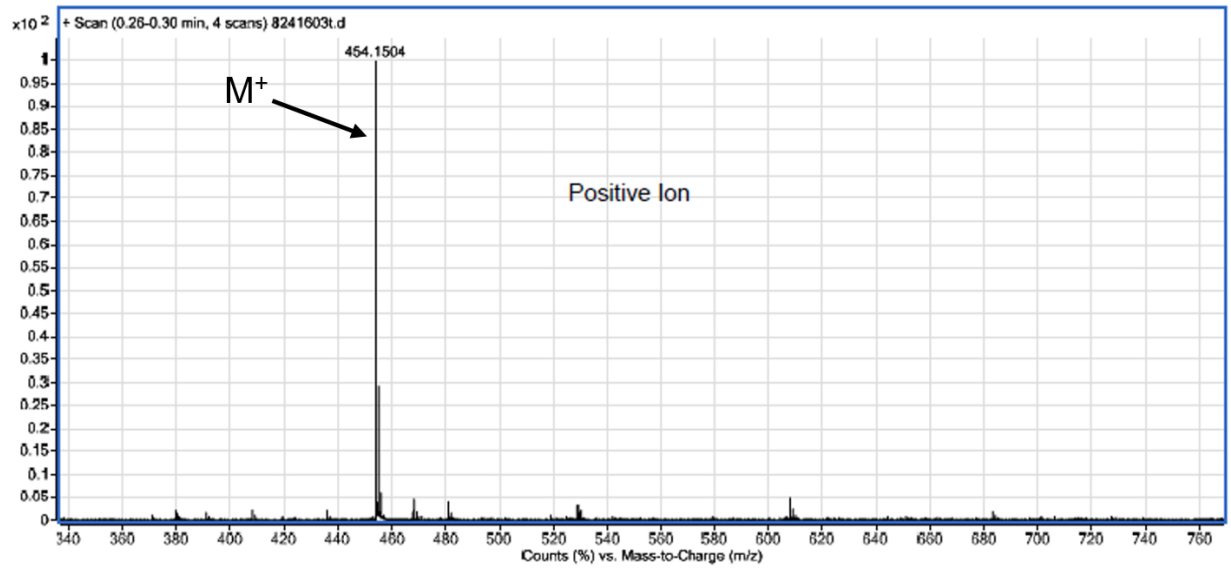

Figure S19. ESI/APCI-MS of illuminated **2.** The identified peak corresponds to the hydrolyzed triphenylphosphonium-containing appendage resulting from ester hydrolysis in **4**.

Photoreactivity of 3 under air; NMR-tube experiment. A solution of **3** (~0.021 mmol) in ~1 mL DMSO-d_6 was placed in an NMR tube under air. An initial ^{1}H NMR spectrum was obtained. This tube was then placed in a Rayonet photoreactor equipped with 419 nm lamps (8 lamps) and illuminated for 24 hours. The solvent was then removed under lyophilization conditions yielding a reddish-brown solid. ^{1}H NMR (DMSO-d_6, 500 Hz) δ 8.69 (s, 1H), 8.23 (d, J = 8.9 Hz, 2H), 8.18 (d, J = 8.5 Hz, 1H), 8.12 (d, J = 8.9 Hz, 2H), 8.01-7.98 (m, 2H), 7.94-7.70 (m, 15H), 7.66-7.62 (m, 2H), 7.55 (t, J = 8.0 Hz, 1H), 7.42 (t, J = 7.9 Hz, 1H), 3.60-3.43 (m, 2H), 1.50-1.30 (m, 7H), 1.28-1.17 (m, 5H) ppm. ESI/APCI-MS (relative intensity) calcd. for $C_{45}H_{43}NO_5PBr$ $[M\text{-}Br]^+$:708.8004; found: 708.3001 (100%).

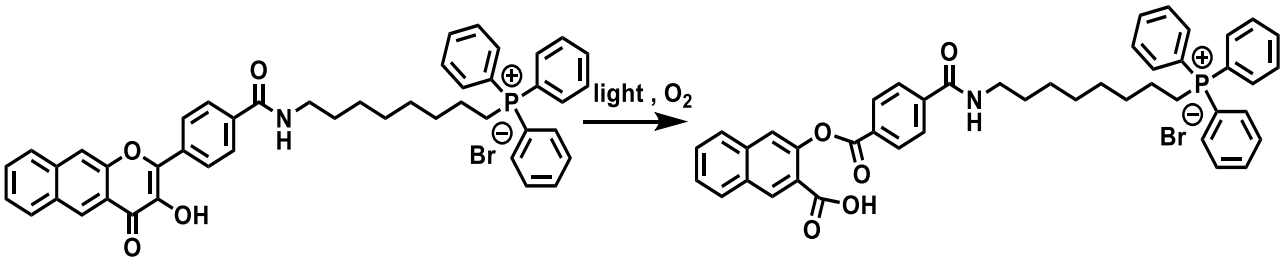

Scheme S5. Photoinduced CO release reaction of **3** to produce **5**.

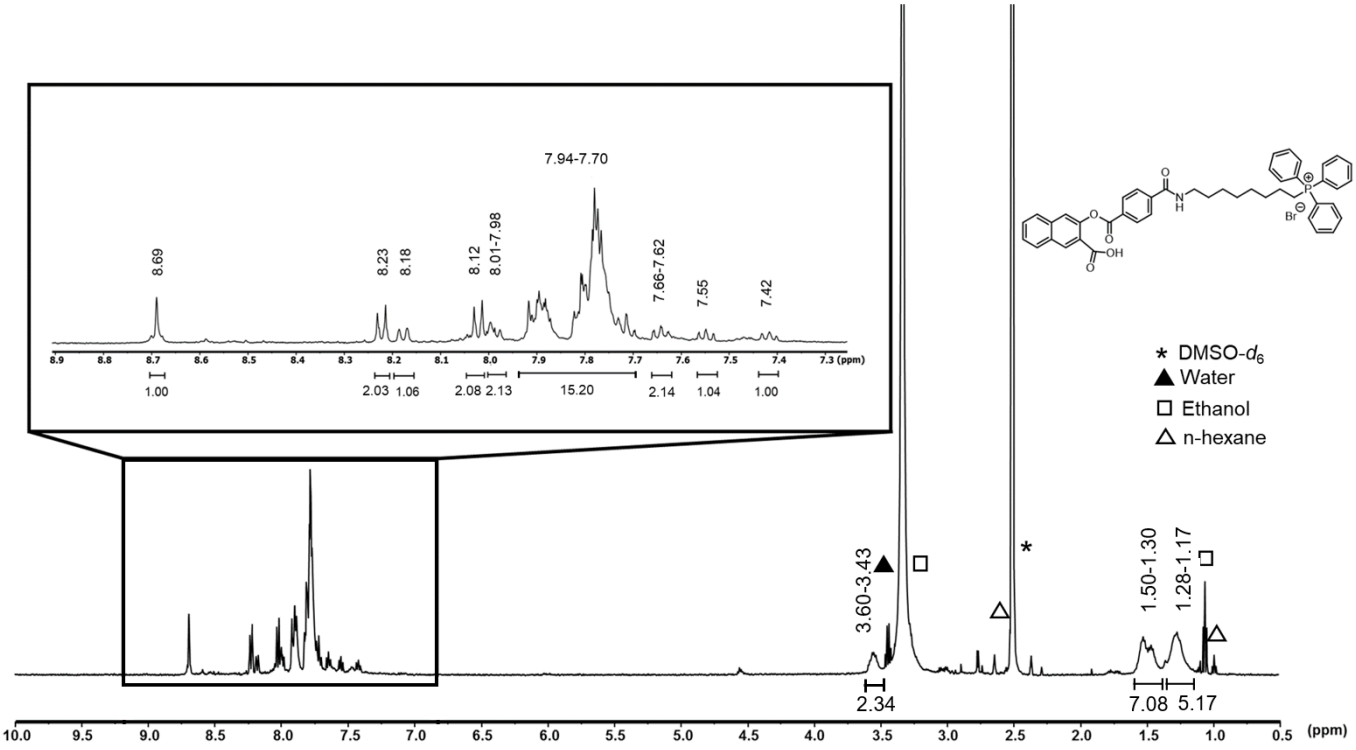

Figure S20. ^{1}H NMR of **3** in DMSO-d_6 illuminated at 419 nm for 24 hours.

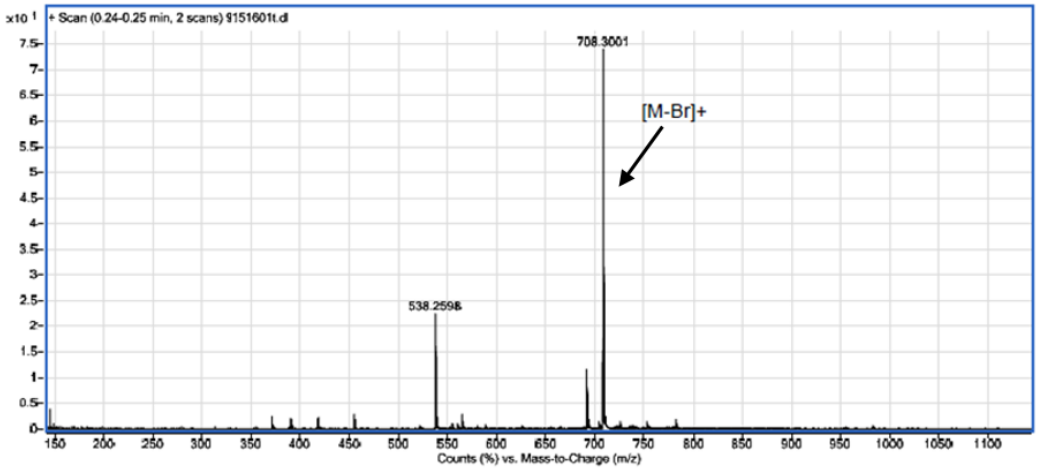

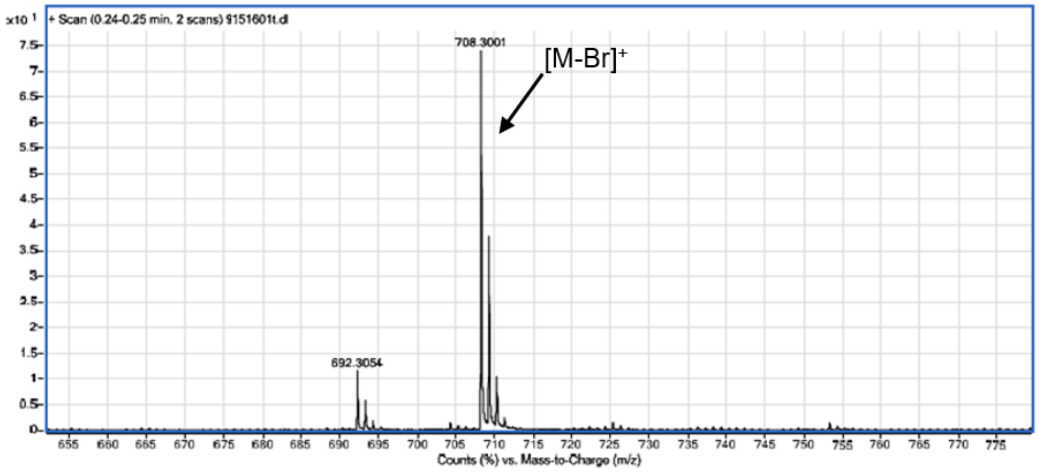

Measured Mass 708.3001

Element	Low Limit	High Limit
C	40	50
H	40	48
N	0	1
O	3	8
P	0	1

Formula	Calculated Mass	mDaError	ppmError	RDB
C46 H45 O5 P	708.3005	-0.4	-0.5	25
C45 H42 N O7	708.2961	4.0	5.6	25.5
C46 H44 O7	708.3087	-8.6	-12.1	25
C42 H47 N O7 P	708.3090	-8.9	-12.6	20.5
C49 H42 N O4	708.3114	-11.3	-15.9	29.5
C45 H43 N O5 P	708.2879	12.2	17.2	25.5
C49 H40 O5	708.2876	12.5	17.7	30
C42 H45 O8 P	708.2852	14.9	21.0	21
C49 H41 O3 P	708.2793	20.8	29.3	30
C50 H44 O4	708.3240	-23.9	-33.7	29

Figure S21. ESI/APCI-MS of **5**.

Dark Control Reaction for compound 2 or 3. A solution of **2** or **3** in DMSO-d_6 (~0.021 M) was prepared in air under minimal red light exposure and placed in an NMR tube. The NMR tube was then covered with foil, placed in a photo reactor, and illuminated using 419 nm lamps for 24 hours. Evaluation of the solution by ^{1}H NMR indicated that no reaction had occurred. That implies that the compound is thermally stable and only undergoes CO release upon photodegradation.

Anaerobic Control Reaction for compound 2 or 3. A solution of **2** or **3** in DMSo-d_6 (~0.021 M) was prepared under N_2 under minimal red light exposure and placed in an NMR tube. The NMR tube was then placed in a photo reactor, and illuminated using 419 nm lamps for 24 hours. Evaluation of the solution by ^{1}H NMR indicated that no reaction had occurred. This implies that the compound only undergoes CO release in the presence of oxygen.

Qualitative analysis of localization of 1 and 2 at 10x via fluorescence microscopy

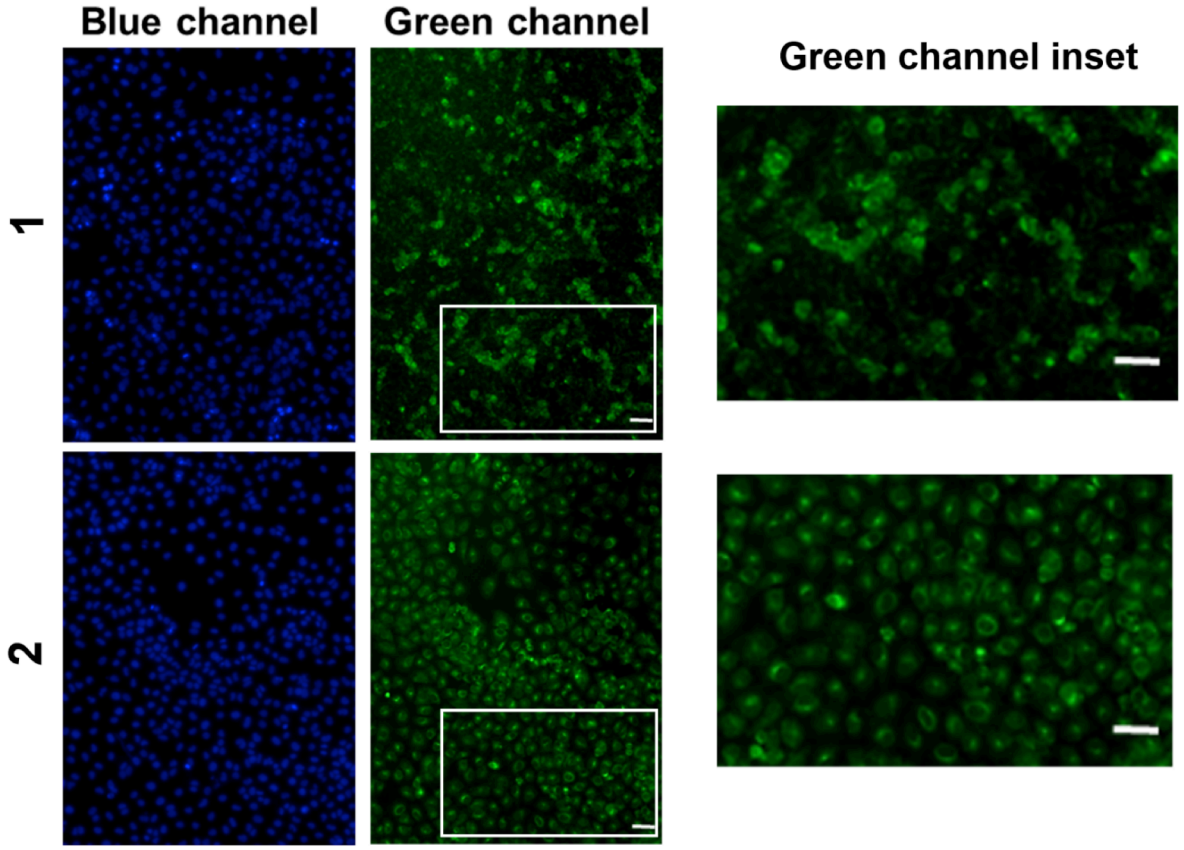

Figure S22A. Individual fluorescence microscopy images of A549 cells incubated for 4 h with compound **1** (50 μM) (row 1), and compound **2** (50 μM) (row 2). Detection of compounds **1** and **2** (shown above as green emissive species) was performed using Zeiss filter set using Zeiss filter set 38: λ_{ex} = 450-490 nm (BP 470/40 filter) and λ_{em} = 500-550 nm (BP 525/50 filter). Cells were co-stained with Hoechst 33342 nuclear dye (blue channel). For localization of Hoechst dye, images were acquired at λ_{ex} = 365 nm and λ_{em} = 420-470 nm (BP 445/50 filter), shown in blue above (repeated down the rows for visual comparison). The inset shown on the right side is a 2x digital zoom. The scale bar on the plot denotes 50 μm.

Qualitative analysis of localization of 1 at 20x via fluorescence microscopy

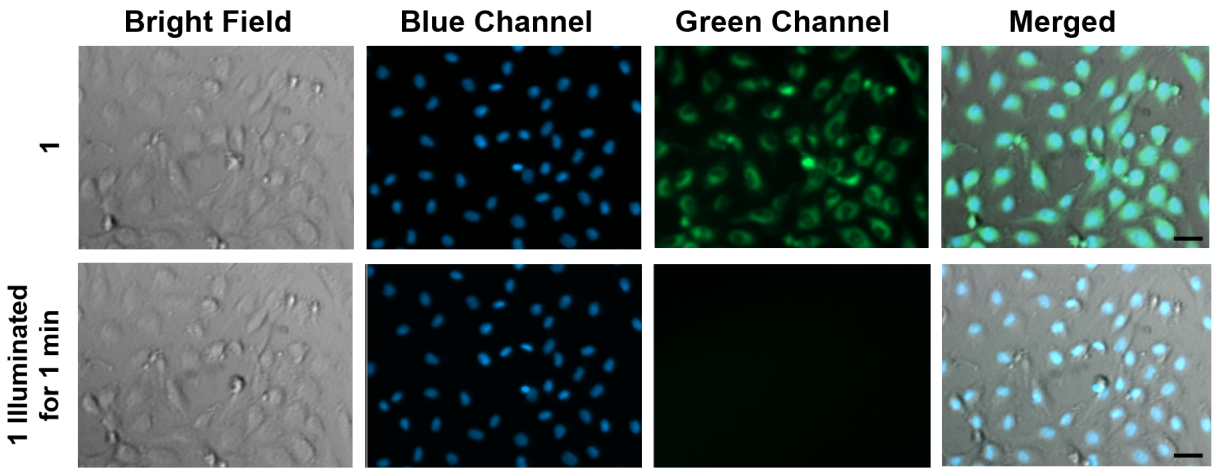

Figure S22B. Individual fluorescence microscopy images of A549 cells incubated for 4 h with compound **1** (50 μM) (row 1), and after illumination (488 nm, 42 620 lx) (row 2). Detection of compound **1** (shown above as green emissive species) was performed using Zeiss filter set using Zeiss filter set 38: λ_{ex} = 450-490 nm (BP 470/40 filter) and λ_{em} = 500-550 nm (BP 525/50 filter). Cells were co-stained with Hoechst 33342 nuclear dye (blue channel). For localization of Hoechst dye, images were acquired at λ_{ex} = 365 nm and λ_{em} = 420-470 nm (BP 445/50 filter), shown in blue above (repeated down the rows for visual comparison). The scale bar on the plot denotes 50 μm.

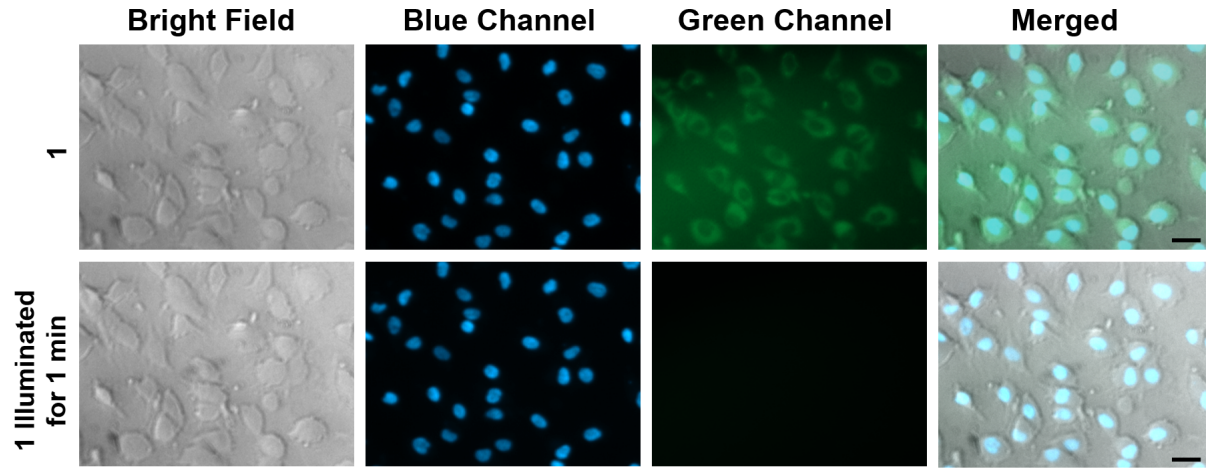

Figure S22C. Individual fluorescence microscopy images of HUVECs incubated for 4 h with compound **1** (50 μM) (row 1), and after illumination (488 nm, 42 620 lx) (row 2). Detection of compound **1** (shown above as green emissive species) was performed using Zeiss filter set using Zeiss filter set 38: λ_{ex} = 450-490 nm (BP 470/40 filter) and λ_{em} = 500-550 nm (BP 525/50 filter). Cells were co-stained with Hoechst 33342 nuclear dye (blue channel). For localization of Hoechst dye, images were acquired at λ_{ex} = 365 nm and λ_{em} = 420-470 nm (BP 445/50 filter), shown in blue above (repeated down the rows for visual comparison). The scale bar on the plot denotes 50 μm.

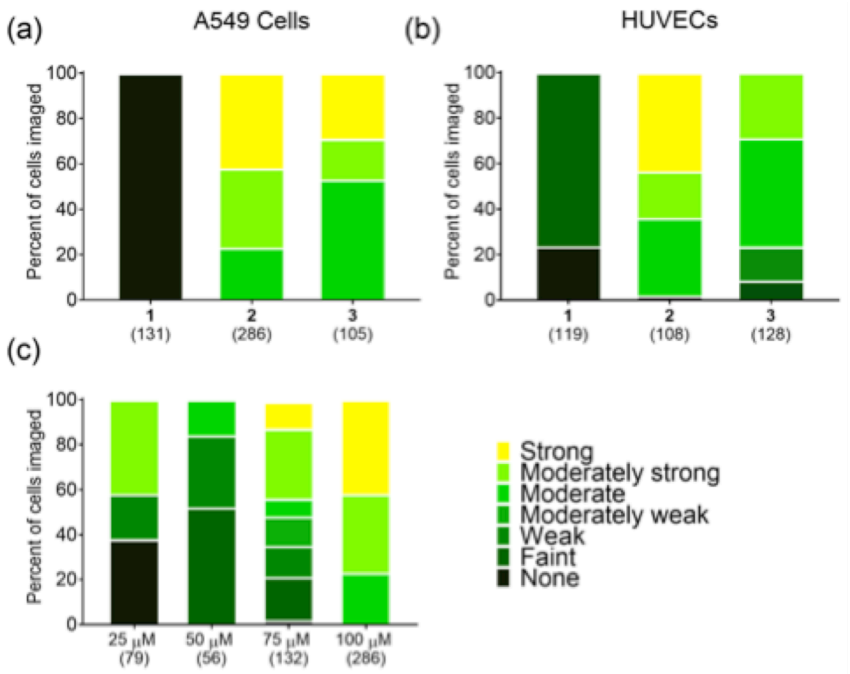

Figure S23. Qualitative assessment of fluorescence emission signal intensity of **1-3** in A549 (a,c) cells and HUVECs (b). Two individuals qualitatively assessed the strength of signal. The numbers of cells imaged for each treatment is indicated in parentheses

Confocal microscopy, cellular uptake of 1-3 in A549 and HUVEC

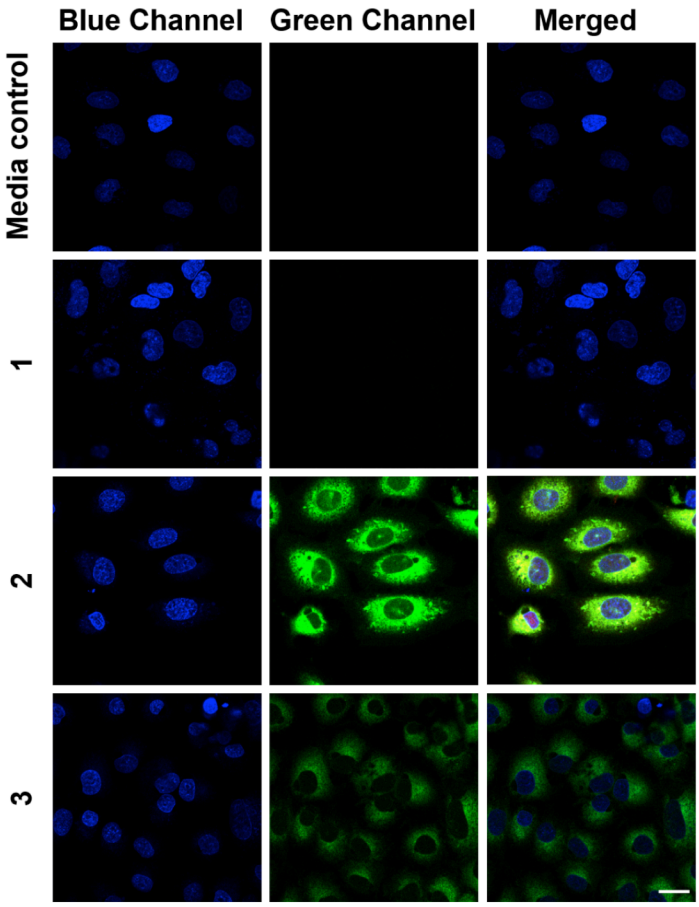

Figure S24. Confocal microscopy depicting cellular uptake of **1**, **2**, and **3** in A549 cells. Cells were treated with vehicle media control (0.4% DMSO) (row 1), 100 μM **1** (row 2), 100 μM **2** (row 3) and 100 μM **3** (row 4) for 4 h. Representative images shown depict the Hoechst 33342 nuclear stain (blue), the CO donor (green) or a merge of the two fluorescence channels. Experiments were repeated at least three times, and a minimum of 21 cells were visualized for each experiment. Scale bar indicates 20 μm.

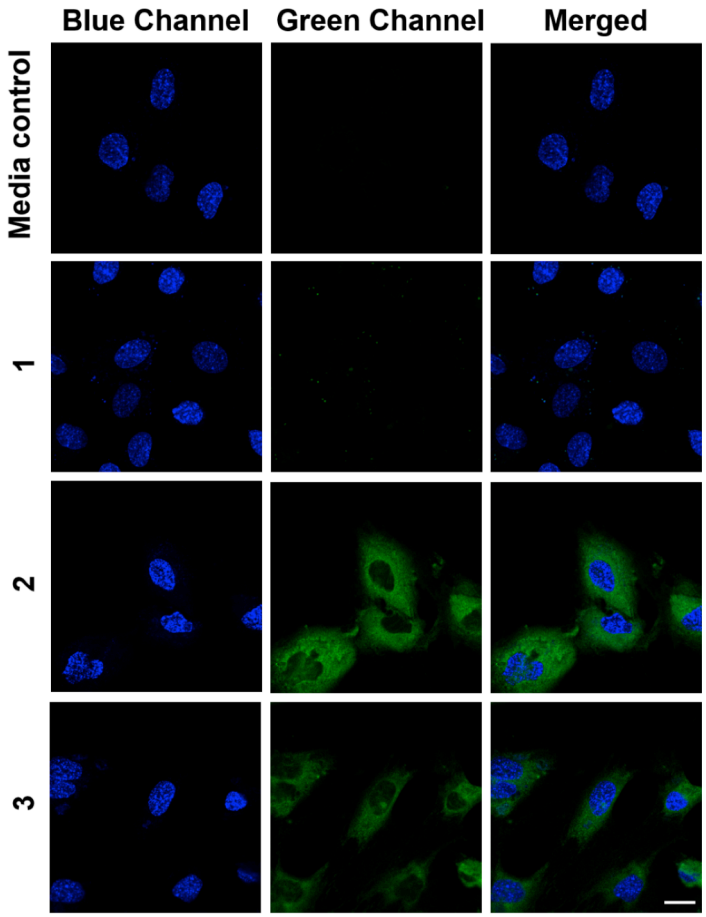

Figure S25. Confocal microscopy depicting cellular uptake of **1**, **2**, and **3** in HUVECs. Cells were treated with vehicle media control (0.4% DMSO) (row 1), 100 μM **1** (row 2), **2** (row 3) and **3** (row 4) for 4 h. Representative images shown depict the Hoechst 33342 nuclear stain (blue), the CO donor (green) or a merge of the two fluorescence channels. Experiments were repeated at least three times, a minimum of 18 cells were visualized for each experiment. Scale bar indicates 20 μm.

Confocal microscopy, co-localization of 2 and 3 in mitochondria of HUVEC and A549 cells

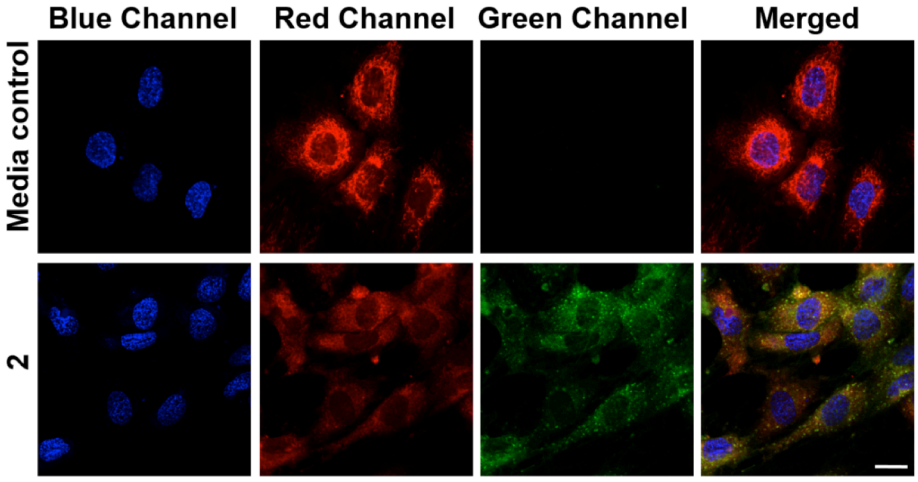

Figure S26. Co-localization of **2** with mitochondria in HUVEC cells. Cells were treated with vehicle control (0.4% DMSO) (row 1), or 100 μM **2** (row 2) for 4 h, then counterstained with Hoechst 33342 and MitoTracker Red CMXRos. Representative images shown depict the Hoechst nuclear stain (blue), the MitoTracker mitochondria stain (red) the CO donor (green) or a merge of the three fluorescence channels. Experiments were repeated at least three times, and at least 18 cells were visualized for each experiment. Scale bar indicates 20 μm.

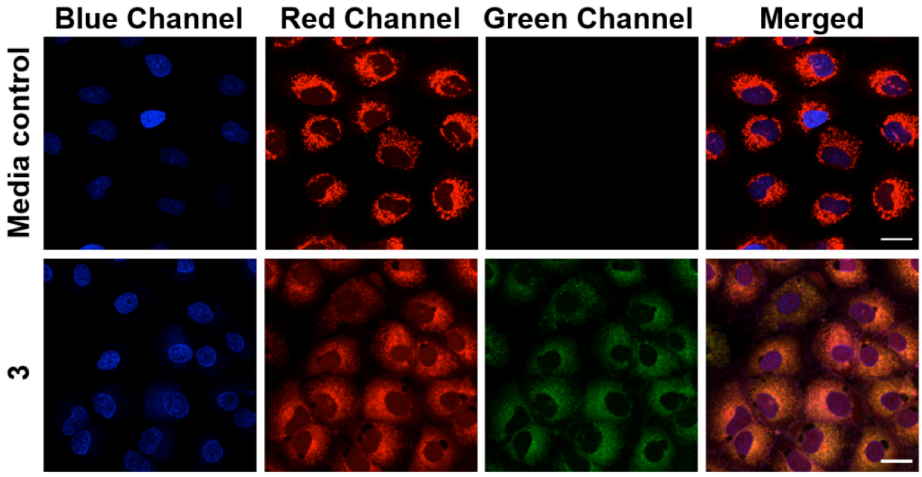

Figure S27. Co-localization of **3** with mitochondria in A549 cells. Cells were treated with vehicle control (0.4% DMSO) (row 1), or 100 μM **3** (row 2) for 4 h, then counterstained with Hoechst 33342 and MitoTracker Red CMXRos. Representative images shown depict the Hoechst nuclear stain (blue), the MitoTracker mitochondria stain (red) the CO donor (green) or a merge of the three fluorescence channels. Experiments were repeated at least three times, and at least 18 cells were visualized for each experiment. Scale bar indicates 20 μm.

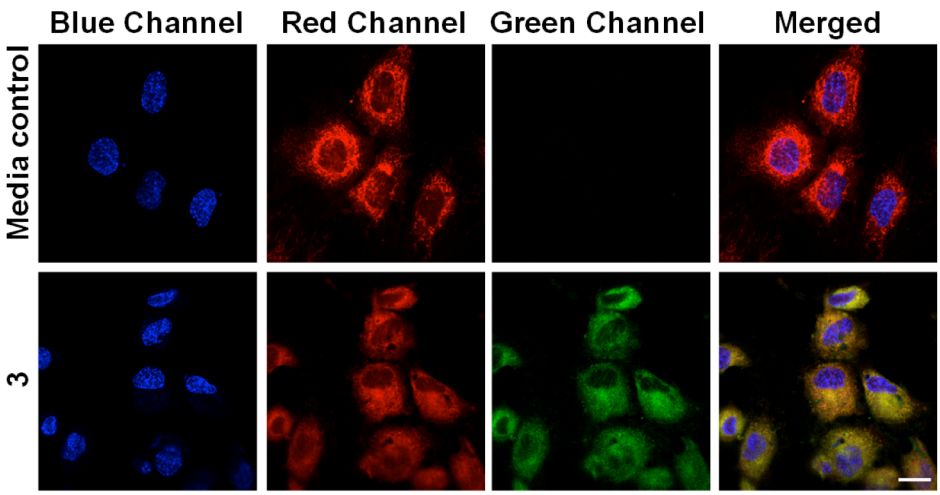

Figure S28. Co-localization of **3** with mitochondria in HUVECs. Cells were treated with vehicle control (0.4% DMSO) (row 1), or 100 μM **3** (row 2) for 4 h, then counterstained with Hoechst 33342 and MitoTracker Red CMXRos. Representative images shown depict the Hoechst nuclear stain (blue), the MitoTracker mitochondria stain (red) the CO donor (green) or a merge of the three fluorescence channels. Experiments were repeated at least three times, and at least 18 cells were visualized for each experiment. Scale bar indicates 20 μm.

CO release studies in mitochondria

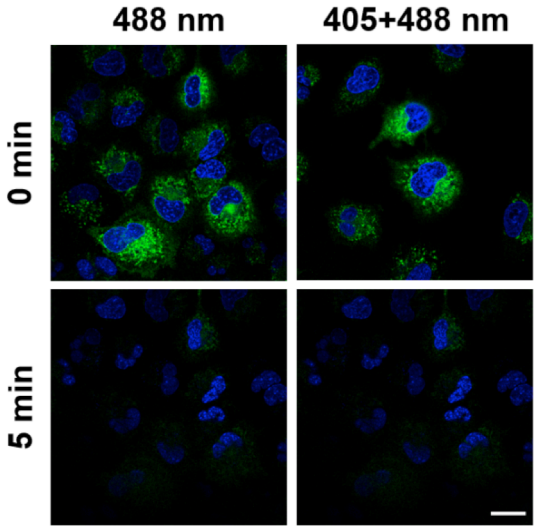

Figure S29. Light induced photodegradation of **2** in A549 cells. The cells were treated with 25 μM **2** in 0.1% DMSO for 4 h, then counterstained with Hoechst 33342 prior to confocal microscopy. After obtaining initial images at wavelengths 410-492 nm for the nuclear stain (blue) and 495-611 nm for the CO donor (green) (row 1), the cells were exposed to light at wavelength 488 nm (row 2, column 1) or 405 and 488 nm (row 2, column 2) (11.5 mW/cm^2 at 6% laser power) for 5 min and then re-imaged. Images are representative of 79 total cells visualized over one experiment. Scale bar indicates 20

Cell Viability Assay (MTT assay) no exposure to light

Cell viability was assessed using the MTT (3-(4,5-dimethylthiazol-2-yl)-2,5-diphenyltetrazolium bromide) assay. MTT (Sigma-Aldrich) was prepared fresh at 5 mg/mL in sterile PBS solution then filtered through a 0.22 μM PES filter. HUVEC or A549 cells were seeded in 96-well tissue treated plates (Corning, NY) at 10,000 cells/well in a volume of 190 μL/well and allowed to attach for 24 hours. The cells were then treated in triplicate wells with concentrations ranging from 80 nM to 100 μM of compound **1**, **2** or **3** and their post-illumination byproducts to a final DMSO concentration that did not exceed 0.4% and incubated for 24 hours. MTT solution (20 μL) was then added to each well, and incubated for 4 more hours. The metabolized formazan pellets were solubilized by adding 200 μL of DMSO and absorption was measured by Modulus™ Microplate reader (Turner Biosystems) at 560 nm and 750 nm (background).

The final results were obtained upon background signal subtraction followed by division of the obtained values by the absorption in the vehicle control (0.4% DMSO) wells. All values were analyzed using GraphPad Prism 7 (La Jolla, California) and reported using Standard Error Mean (SEM). IC_{50} values were calculated using a nonlinear regression (curve fit) with a bottom constraint of zero. All experiments were performed in triplicate under dark conditions.

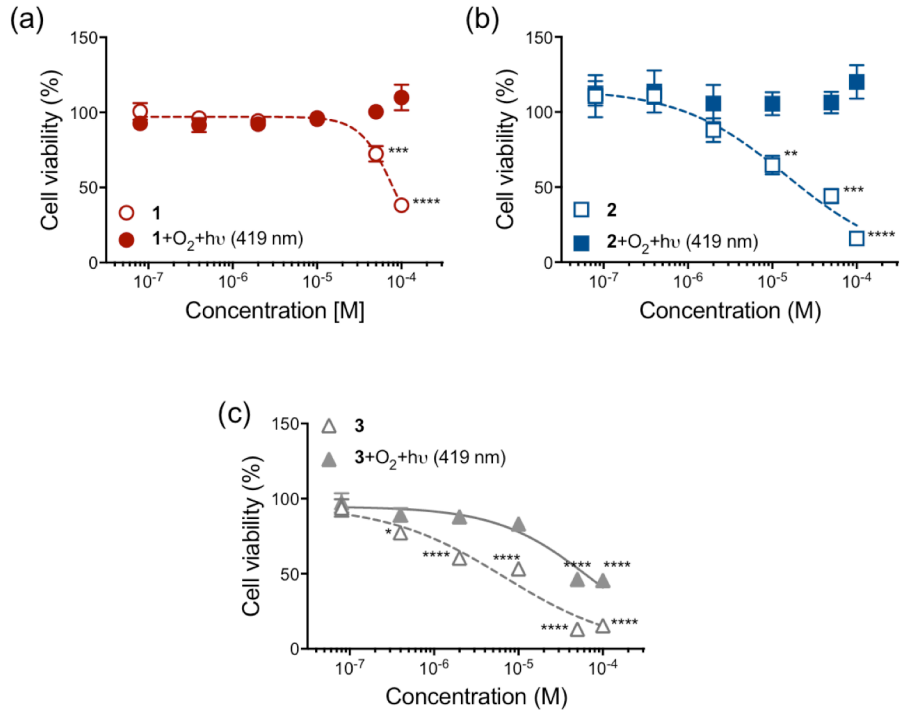

Figure S30. Plots of human adenocarcinomic alveolar basal epithelial cells (A549) percent cell viability versus concentration for **1** (A), **2** (B), or **3** (C) and their photoinduced reaction products. IC_{50} values were determined using a four-parameter nonlinear regression for assays wherein at least a 50% reduction in cell viability was observed. Values shown are the mean ± SEM percent viability of cells with respect to the control (0.4% DMSO). Cell viability data and non-linear regression analyses (four-parameter, variable slope) are shown for the native compounds (open symbols, dashed lines) and their photo-degraded products (closed symbols, solid lines). Error bars not visible are smaller than the symbol size. Panel A, n = 6 replicate experiments; panels B-C, n = 3 replicate experiments. *, $p<0.05$; **, $p<0.01$; ***, $p<0.001$; ****, $p<0.0001$ as determined by one-way ANOVA for each compound as compared to lowest concentration tested, 0.08 μM.

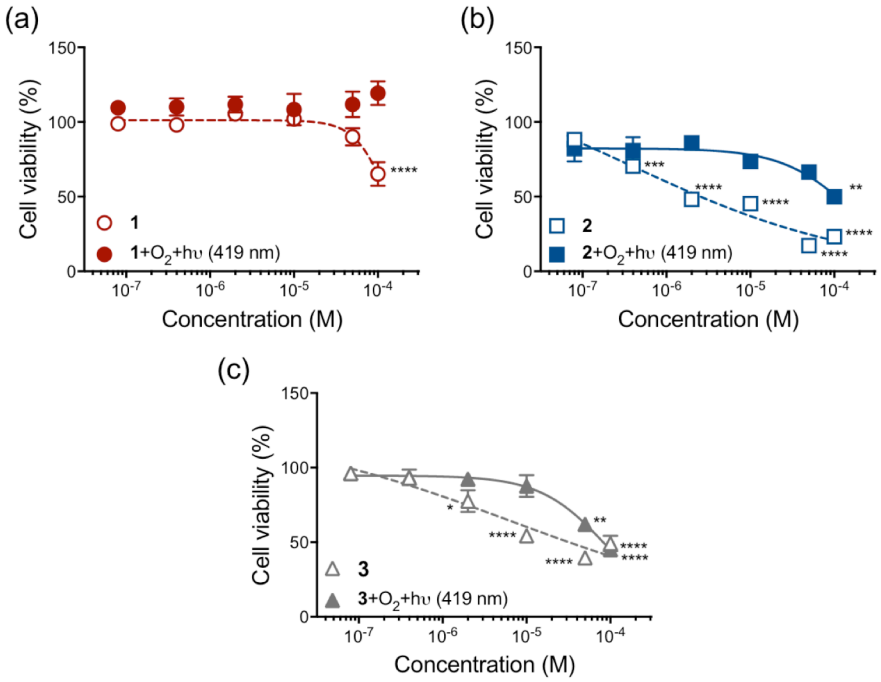

Figure S31. Plots of human umbilical vein endothelial cells (HUVECs) percent cell viability versus concentration for **1** (A), **2** (B), or **3** (C) and their photoinduced reaction products. IC_{50} values were determined using a four-parameter nonlinear regression for assays wherein at least a 50% reduction in cell viability was observed. Values shown are the mean ± SEM percent viability of cells with respect to the control (0.4% DMSO). Cell viability data and non-linear regression analyses (four-parameter, variable slope) are shown for the native compounds (open symbols, dashed lines) and their photo-degraded products (closed symbols, solid lines). Error bars not visible are smaller than the symbol size. Panel A, n = 6 replicate experiments; panels B-C, n = 3 replicate experiments. *, $p<0.05$; **, $p<0.01$; ***, $p<0.001$; ****, $p<0.0001$ as determined by one-way ANOVA for each compound as compared to lowest concentration tested, 0.08 μM.

Table S1. Calculated IC_{50} values for **1**, **2**, and **3** in A549 and HUVEC cells determined by the MTT Assay without exposure to light.

Cell line	**1**	**1**+O_2+hν	**2**	**2**+O_2+hν	**3**	**3**+O_2+hν
A549	80.2±3.3	ND	14.1±2.7	ND	8.48±4.0	69.1±11
HUVEC	L	ND	1.51±1.4	L	8.40±3.6	90.0±7.5

IC_{50} values were calculated by non-linear regression analysis (four-parameter, variable slope) was performed (GraphPad Prism v. 7, La Jolla, CA) to generate the concentration-response curve for each chemical using each cell line. Values represent the mean ± SEM (n = 3 independent experiments, except n = 6 for **1** in A549 cells). ND, no significant decrease in cell viability; L, less than 50% decrease in cell viability.

Cell Viability Assay (MTT assay) including the exposure to light to induce CO release in situ

Three independent biological experiments, each with three technical replicates, were performed for **1**, **2**, **4** and TPP under visible light-induced CO release conditions. HUVECs or A549 cells were seeded in 96-well plates (Corning, NY) at 10,000 cells/well for 24 h. The cells were then treated with **1**, **2**, **4** and TPP at 0.08-100 μM with a final DMSO concentration that did not exceed 0.4%. For visible light-triggered in situ CO release, the plates were exposed to blue LEDs for 1 h and incubated for an additional 23 h. After 24 h, MTT solution (20 μL) was added and the cells were incubated for an additional 4 h. The metabolized formazan pellets were solubilized by adding 200 μL of DMSO and absorption values were measured using a Modulus™ Microplate reader (Turner Biosystems) at 560 and 750 nm. The final results were background subtracted and normalized to vehicle control (0.4% DMSO). Data analysis was performed using GraphPad Prism 7 (La Jolla, California), with values reported as mean ±SEM. IC_{50} values were calculated as nonlinear regression with a bottom constraint of zero.

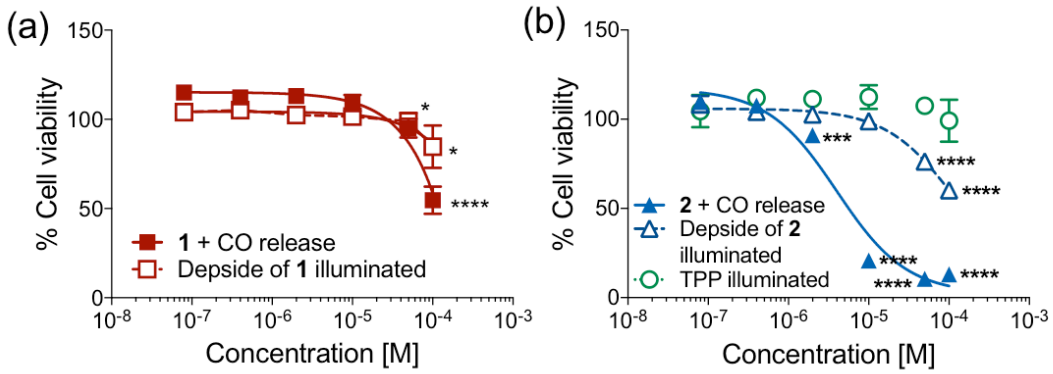

Figure S32. Plots of human umbilical vein endothelial cells (HUVECs) percent cell viability versus concentration for **1** (A), or **2** (B) and their photoinduced reaction products as well as TPP control upon illumination in cells. IC_{50} values were determined using a four-parameter nonlinear regression for assays wherein at least a 50% reduction in cell viability was observed. Values shown are the mean ± SEM percent viability of cells with respect to the control (0.4% DMSO). Cell viability data and non-linear regression analyses (four-parameter, variable slope) are shown for the native compounds (open symbols, dashed lines) and their photo-degraded products (closed symbols, solid lines). Error bars not visible are smaller than the symbol size. Panel A, and B n = 3 replicate experiments. *, $p<0.05$; **, $p<0.01$; ***, $p<0.001$; ****, $p<0.0001$ as determined by one-way ANOVA for each compound as compared to lowest concentration tested, 0.08 μM.

Table S2. Calculated IC_{50} values for **1**, **2** and TPP in A549 and HUVEC cells determined by the MTT Assay upon exposure to visible light.

Cell line	**1**	**1**+O_2+hν	**2**	**2**+O_2+hν	**TPP**+O_2+hν
A549	76.1±5.2	ND	4.6±3.6	ND	ND
HUVEC	L	ND	3.78±1.5	L	ND

IC_{50} values were calculated by non-linear regression analysis (four-parameter, variable slope) was performed (GraphPad Prism v. 7, La Jolla, CA) to generate the concentration-response curve for each chemical using each cell line. Values represent the mean ± SEM (n = 3 independent experiments). ND, no significant decrease in cell viability; L, less than 50% decrease in cell viability.

Bioenergetic analysis in cultured cells

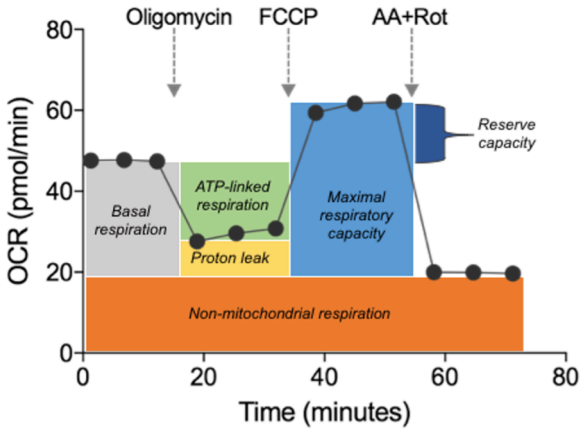

Scheme 6. Schematic representation of OCR adapted from Agilent Technologies.

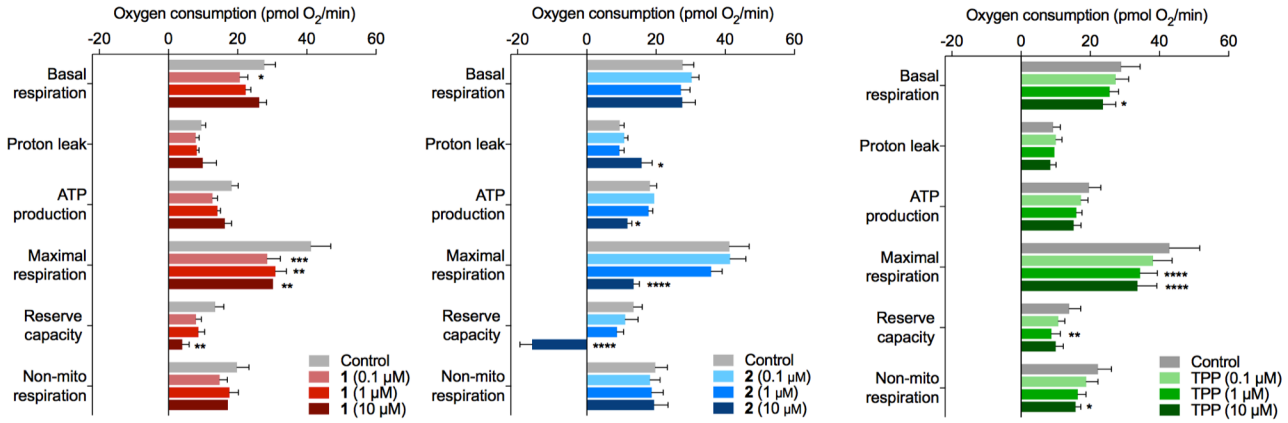

Figure S33. Cellular bioenergetics analysis in A549 cells (no light exposure). Data displayed show basal respiration, proton leak, ATP production, maximal respiration, and non-mitochondrial respiration in the presence of **1** (blue colors), **2** (yellow colors) and TPP tail (green colors) at the 0.1-10 μM concentration range. Abbreviations: FCCP, carbonyl cyanide 4-(trifluoromethoxy)phenylhydrazone; AA+Rot, antimycin A and rotenone. Values represent the means ± SEMs from three independent biological experiments each with eight technical replicates. The values that are significantly different by one-way ANOVA test are indicated by asterisks as follows: *p < 0.05, **p < 0.01, ***p < 0.001, *****p < 0.0001.

Compound	[CORM]/μM	Basal	ATP-linked	Proton-leak Linked	Maximal Respiration	Reserve Capacity	Non mitochondrial
CORM-401[a]	10	No significant difference compared to control					
	30	↑	↓	↑	↓	↓	↑
	100	↑	↓	↑	↓	↓	↑
iCORM-401[a]	10-100	No significant difference compared to control					
CORM-401[b]	5	No significant difference compared to control					
	10	No significant difference compared to control					
	50	↑	↓	↑	↓	↓	↑
	100-500	Toxic					
iCORM-401[b]	10-100	No significant difference compared to control					
CORM-2[c]	50	No significant difference compared to control					
	100	↑	↓	↑	↓	↓	↑
	250	↑	↓	↑	↓	↓	↑
	500	Toxic					
CORM-3[d]	1	No significant difference compared to control					
	20	Performance of Complex I, II, II were not affected by 20 and 100 μM of CORM-3 and 100 μM of iCORM-3. Inhibition of complex IV was observed only at 100 μM of CORM-3.					
	100						
iCORM-3[d]	100	No significant difference compared to control					
1	0.1	No significant difference compared to control					
	1						
	10	↓	↓	---	↓	↓	---
2	0.1	No significant difference compared to control					
	1						
	10	↓	↓	---	↓	↓	---

Figure S34. Summary of bioenergetics studies performed using CORM-401, CORM-2 and CORM-3 measured using Seahorse XF instrument.

[a]Kaczara, P.; Motterlini, R.; Rosen, G.M.; Augustynek, B.; Bednarczyk, P.; Szewczyk, A.; Foresti, R.; Chlopicki, S. *Biochim. Biophys. Acta* **2015**, *1847*, 1297-1309.
[b]Wilson, J.L.; Bouillaud, F.; Almeida, A.S.; Vieira, H.L.; Ouidja, M.O.; Dubois-Randé, J.L.; Foresti, R.; Motterlini, R. *Free Radic. Biol. Med.* **2017**, *104*, 311-323.
[c]Reiter, C.E.N.; Alayash, A.I. *FEBS Open Bio.* **2012**, *2*, 113-118.
[d]Iacono, L.L.; Boczkowski, J.; Zini, R.; Salouage, I.; Berdeaux, A.; Motterlini, R.; Morin, D. *Free Radic. Biol. Med.* **2011**, *50*, 1556-1564.

List of CORMs shown in Figure S34 and their chemical structure:

CORM-401: 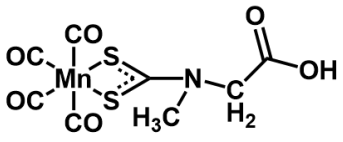

CORM-3: 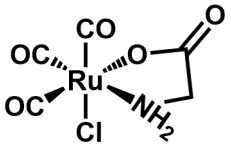

CORM-2: 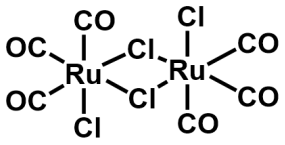

References

1. Fletcher, D.I.; Ganellin, C.R.; Piergentili, A.; Dunn, P.M.; and Jenkinson, D.M. *Bioorg. Med. Chem.* **2007**, *15*, 5457-5479
2. Anderson, S.N.; Richards, J.M.; Esquer, H.J.; Benninghoff, A.D.; Arif, A.M.; Berreau, L.M. *ChemistryOpen* **2015**, *4*, 590-594.
3. Rahman, S.M.A.; Baba, T.; Kodama, T.; Islam, Md. A.; Obika, S. *Bioorg. Med. Chem.* **2012**, *20*, 4098-4102.